JOURNAL OF MATERIALS SCIENCE **40** (2005) 3169–3176

# Comparison of the intergranular segregation for eight dilute binary metallic systems in the $\Sigma 11'$ {332} tilt grain boundary

O. HARDOUIN DUPARC*
*LSI, École Polytechnique, 91128 Palaiseau Cedex, France*
*E-mail: olivier.hardouinduparc@polytechnique.edu*

A. LARERE
*LEMHE, Université de Paris XI, 91405 Orsay Cedex, France*

B. LEZZAR, O. KHALFALLAH
*LMDM, Mentouri University, Constantine, Algeria*

V. PAIDAR
*Institute of Physics, Academy of Sciences, Na Slovance 2, Prague, Czech Republic*

Intergranular segregation is studied in the limit of infinitely diluted solution for eight dilute metallic systems made of four face centred cubic metals, one transition metal, nickel, and three noble metals, copper, silver and gold. The grain boundary (GB) chosen is the symmetrical tilt $\Sigma = 11'$ {332} ⟨110⟩ GB with its characteristic "zigzag" structural pattern as numerically calculated and experimentally observed by high resolution transmission electronic microscopy in nickel. The metallic interactions are modelled with Finnis-Sinclair like potentials. The atomic sites are characterised by a geometrical parameter defined with their exact Voronoï' volumes and the tensor of the stresses locally exerted. The {332} GB presents the most diversity of sites in these respects. The segregation energies are computed and analysed versus the only two 'driving forces' which can play a role in metallic intergranular segregation, viz. the elastic size effect and the excess cohesion energy effect. The elastic size effect calculated by the method of virtual impurity represents the main segregation driving force in most cases of the considered systems. It is worth noting however that the excess cohesion energy effect is important for non hydrostatic or compressive sites. It can even be predominant, as in the case of Ni(Cu).
© *2005 Springer Science + Business Media, Inc.*

## 1. Introduction

Intergranular segregation by dopants or impurities has a crucial rôle on all physical, chemical and mechanical properties of polycrystalline materials that depend on the nature of their grain boundaries, such as grain growth, corrosion and fracture. Review articles already exist [1–6], together with many numerical simulation studies at the atomic scale [7–24].

One possible approach to try to better understand the physics of segregation is to identify its "driving forces". Three such "driving forces" have been identified for surface segregation on metals using phenomenological models of interaction. They can be termed as a size effect, an excess cohesion effect and an alloy effect [25–28]. The relative contributions of these three driving forces has also been investigated numerically for the intergranular segregation of silver in copper and copper in silver for the two symmetric $\Sigma = 5$ ⟨001⟩ tilt grain boundaries (GBs) [21, 22]. The elastic size effect has been found to be the dominant effect. We refined the level of analysis by studying the only two possible driving forces identifiable for intergranular segregation in the infinite dilution limit, viz. the size effect and excess cohesion effect, in the case of silver in nickel and nickel in silver for the two symmetric $\Sigma = 11$ ⟨110⟩ tilt GBs [24] whose structures had been experimentally observed in nickel. Characterizing the atomic sites in the pure metal GB with two parameters (see Section 2.3), a geometrical one involving the exact Voronoï' volume, and a more physical parameter involving both the local forces and the local distances, viz. the pressure, we found a non negligible contribution of excess cohesion energy in these two systems for sites either characterized by a strong compression or found to be non hydrostatic (but the atomic stress tensor components were not explicitly given in that article).

In this study we want to extend the previous analysis to other dilute binary metallic systems, another system

*Author to whom all correspondence should be addressed.

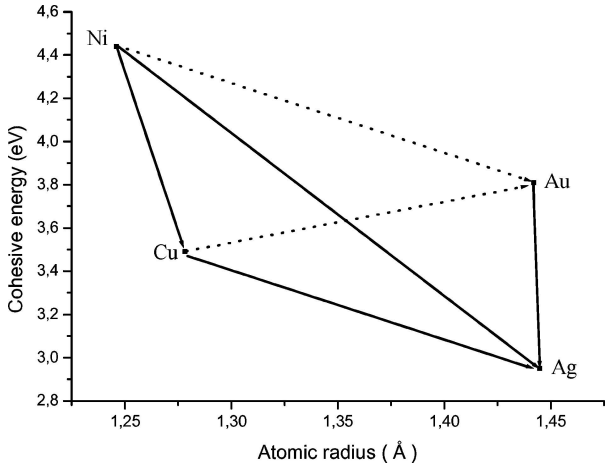


*Figure 1* Cohesive energy $E_c$ (eV) versus fcc atomic radius $r$ (Å) for Nickel, Copper, Silver, and Gold. The atomic radius $r$ is related to the cubic lattice parameter a via $r = a/(2\sqrt{2})$. Experimental values are from [34], see Table I. The continuous lines between metals indicate the binary systems explicitly discussed in this paper.

for which the size effect also ought to be important, Cu-Ag, and two systems for which the size effect should be small, Ni-Cu, or even negligible, Au-Ag. These last two systems should allow for a finer analysis of the cohesion effect in the absence of an overwhelming elastic size effect. One can also note that nickel is a transition metal while copper is a noble metal so that behaviour differences might be expected between Ni-Ag and Cu-Ag for instance. The Ni-Ag and Cu-Ag systems are characterized by a very strong tendency to decomposition [29, 30] primarily due to the difference in size between the atoms of solvent and solute in fcc structure (the first Hume-Rothery rule [31]). They present very small limits of solubility on both sides of the miscibility gap and thus a strong tendency of segregation. The Ni-Cu and Au-Ag systems are miscible.

A synoptic presentation of the cohesive energies and atomic radii of the four face centred (fcc) metals retained, namely nickel, copper, silver and gold, is given in Fig. 1. As explicit in Section 2.1, modelling adapted to fcc metals is carried out using semi-empirical n-body potentials with the now famous negative square root embedding functional [32, 33]. The potentials are adjusted to well reproduce the principal physical characteristics of each metal and alloy.

The eight following binary systems solvent-solute, Ni(Ag), Cu(Ag), Ni(Cu), Au(Ag), and their reverse, Ag(Ni), Ag(Cu), Cu(Ni), Ag(Au), will thus be studied in the limit of the infinitely diluted solutions. The difference in size between atoms is evaluated by the ratio of the atomic radii of the solute (or Impurity I), $r_I$, and solvent (or Matrix $M$), $r_M$, $r = r_I/r_M$. System $M(I)$ will be called 'direct' if this $r$ ratio is higher than 1 and 'reverse' if $r$ is lower than 1. For instance, for Ni(Ag), $r = 1.16$, and for Ag(Ni), $r = 0.862$. Ranging the systems by decreasing order of $r$, one has Ni(Ag), Cu(Ag), Ni(Cu), Au(Ag), Ag(Au), Cu(Ni), Ag(Cu) and Ag(Ni). We shall not explicitly consider here the Ni-Au and Cu-Au systems because they are expected to (and indeed proved to) behave very similarly to the Ni-Ag and Cu-Ag systems.

In our previous article [24], we studied two GBs whose structure had been unambiguously confirmed at the atomic level thanks to HRTEM observations in nickel, the $\Sigma 11$ {113} and the $\Sigma\, 11'$ {332}, and we had found that the latter one contained the most diversity as far as type of atomic sites is concerned with respect to the former one since it included for instance a strongly compressed site absent in the higly symmetric atomic structure of the {113}. We shall thus concentrate here on the $\Sigma 11'$ {332} structure only (see Section 3.1).

## 2. Theory and method

### 2.1. Potentials

Let us first recall the standard outer electronic configurations of the atoms we shall consider in the metallic state: nickel has $3d^8 4s^2$, copper $3d^{10} 4s^1$, silver $4d^{10} 5s^1$, and gold $4f^{14} 5d^{10} 6s^1$.

The potentials we use pertain to the embedded atom philosophy [35] with the Finnis-Sinclair (FS) square root embedding functional [32]. Although originally derived for transition metals [36] this functional proved to be particularly efficient for noble metals as well [33, 37]. The parametrised functions are short ranged exponentials smoothly extended to zero values by adapted polynomials (RGL) [24, 33]. No long range Friedel oscillation term is included.

The cohesion energy of a system containing $N$ atoms with respect to the $N$ atoms being isolated is written as the sum of cohesive embedded terms and repulsive pair interactions. We have

$$E_N = \sum_{i=1}^{N} \left\{ f^{\text{emb}}(\rho_i) + \sum_{j \neq i} E^{\text{rep}}(r_{ij}) \right\}; \quad \text{with}$$

$$f^{\text{emb}}(\cdot) \equiv -\sqrt{(\cdot)}; \rho_i(r) = \sum_{j \neq i} \beta^2(r_{ij}) \text{ and:}$$

$$\beta(r) = \xi e^{-q\left(\frac{r}{r_o}-1\right)} \text{ from } r = 0 \text{ to } r_{c1}, \text{ then smoothly splined to zero at } r = r_{c2} \text{ with a fifth order polynomial,}$$

$$E^{\text{rep}}(r) = A e^{-p\left(\frac{r}{r_o}-1\right)} \text{ from } r = 0 \text{ to } r_{c1}, \text{ then smoothly splined to zero at } r = r_{c2} \text{ with a fifth order polynomial,} \quad (1)$$

$r_o$ is the equilibrium distance between the first neighbours for the considered metal. The energetic parameters $A$ and $\xi$ are deduced exactly from the choice of $p$ and $q$ and the experimental cohesion energy and equilibrium lattice parameter [34]. The dimensionless parameters $p$ and $q$ are adjusted to well reproduce for each metal the elastic constants [34], the Rose universal curve [38] and the vacancy formation energy [39]. The fifth order polynomials defined between $r_{c1}$ and $r_{c2}$ avoid discontinuities in the energies and divergences in the forces [33]. The radii $r_{c1}$ and $r_{c2}$ are chosen such as $r_{o,n} < r_{c1} < r_{c2} < r_{o,n+1}$, where $r_{o,n}$ is the equilibrium distance between the $n$th neighbours and thus define an FS-RGLn potential. Although they have no effect on the equilibrium conditions and elastic constants, they obviously have a significant influence on energies of complex structural defects such as grain

TABLE I Parameters used in the FS-RGL3 potentials defined in the text [24, 32, 33], together with calculated and experimental (figures in parentheses) data for the four metals, '$a$' is the cubic lattice parameter [34]. $E_c$ is the cohesive energy per atom of the perfect crystal [34] while $E_v$ is the formation energy of a vacancy. Experimental $E_v$ are from [39]. Calculated $E_v$ correspond to the unrelaxed vacancy defect. Relaxation only lowers these values by 1 to 2%. $B$ is the bulk modulus and $c_{11}$, $c_{12}$, $c_{44}$ are the three cubic elastic constants, the experimental values correspond to room temperature values [34]. $c' = (c_{11} - c_{12})/2$ is the Coulomb shear constant. $\gamma_t$ is the interfacial energy of the coherent twin fault. We use $\gamma_t \sim \gamma_i/2$ when only the intrinsic stacking fault energy $\gamma_i$ can be found in the literature [40–42].

| Metal | Ni | Cu | Ag | Au |
|---|---|---|---|---|
| $P$ | 10.78 | 9.33 | 10.23 | 10.42 |
| $q$ | 2.50 | 2.80 | 3.38 | 4.00 |
| $r_{c1}/r_o$ | 1.768 | 1.768 | 1.732 | 1.732 |
| $r_{c2}/r_o$ | 1.98 | 1.98 | 2.0 | 2.0 |
| $a$ (Å) | 3.524 | 3.615 | 4.0862 | 4.0786 |
| $E_c$ (eV/at) | 4.44 | 3.49 | 2.95 | 3.81 |
| $E_v$ (eV) | 1.55 (1.79) | 1 (1.22) | 0.77 (1.12) | 0.77 (0.95) |
| $B$ (Gpa) | 203.1 (183.7) | 141.8(137) | 108.3 (103.8) | 168.4(172.8) |
| $c'$ (Gpa) | 37.5 (50.3) | 20.2 (23.5) | 15 (15.15) | 18.4(14.6) |
| $c_{11}$ (Gpa) | 253 (250.8) | 168.8 (168.4) | 128.2 (124) | 192.9 (192.3) |
| $c_{12}$ (Gpa) | 178.1 (150.2) | 128.3 (121.4) | 98.3 (93.7) | 156.1(163.1) |
| $c_{44}$ (Gpa) | 111.3(123.5) | 63.4 (75.4) | 42.9 (46.1) | 49.3 (42) |
| $\gamma_t$ (mJ/m$^2$) | 42 (∼58) | 21 (16−25) | ∼5 (∼8) | ∼2 (∼16) |

boundaries. They are adjusted so as to reproduce estimated excess energy $\gamma_t$ of the twin $\Sigma = 3\,\{1\,1\,1\}\,\langle 1\,10\rangle$ [40–42].

We follow a procedure already used for Ni-Au [43] for the crossed M-I interactions. The crossed parameters A and $\xi$, are obtained as geometric means of the corresponding parameters for the M-M and I-I interactions, and the crossed $p$, $q$, $r_{c1}$ and $r_{c2}$ parameters are similarly obtained as arithmetic means.

Parameters and results obtained for our FS-RGL3 potentials are given and compared to experimental data in Table I. It is probably the main quality of the $n$-body potentials to give a correct estimation of the vacancy formation energies (Pair potentials give an unrelaxed formation energy equal to the atomic cohesive energy, which is obviously wrong for metals). Let us note that $\gamma_t$ would be zero for FS-RGL2 potentials and can even be slightly negative because of the cutoff polynomials.

The bulk modulus B measures the hydrostatic 'compressive' response. Nickel is the least compressive metal. The two shear constants $c'$ and $c_{44}$ measure the energy responses to imposed angular distortions. One can see that in this respect nickel is much more rigid than copper, gold and silver, by factors from two to three. This corresponds to the fact that nickel is the only transition metal among the four metals considered here. Its binding due to its d-electrons is angular dependent because of the directionality of the d-orbitals. Even if our FS-RGL potential does not explicitly contain this feature, it still has it somehow implicitly via the fitting of the potential parameters on the elastic properties of the material.

Let us finally mention that nickel is ferromagnetic below $T_{\text{Curie}} = 641$ K, a feature we do not explicitly take into account. Gold is special because of its Super Van der Waals interaction between the closed shells of gold atoms due to unmasked relativistic effects [44, 45], another feature we could not either explicitly include in our modelisation. Only ab initio calculations based on the Dirac equation, as opposed to the Schrödinger equation, could do better from that point of view.

## 2.2. Simulation techniques

The systems are relaxed by means of a quenched molecular dynamics algorithm which leads to the energy minimization at $T = 0$ K [46]. The simulation boxes include several hundreds of atoms. For the study of intergranular segregation, they contain only one grain boundary thanks to the use of Möbius, or antiperiodic, border conditions [47]. These border conditions make it possible to exclude the second grain boundary required by the periodic boundary conditions, and thus to double the distance which separates the grain boundary from its image.

## 2.3. Local stresses, pressures and Voronoï volumes

On can define at the atomic level the Kluger stress density tensor $\vec{\vec{\tau}}_i$ associated to an atom $i$ which undergoes $\mathbf{f}_{ij}$ forces from its $j$ neighbours. The average of the diagonal components of this tensor corresponds to a local atomic (density) pressure, withstanding a change of sign to comply with the conventional definition of a pressure. A negative pressure $p_i$, corresponds to a site in tension and the positive pressure corresponds to a site in compression. One caveat concerning the use of this atomic (density) pressure is that this scalar value is really significant only if the non diagonal components of the stress tensor are negligible and if the three diagonal components are roughly equal. One has [5, 48]:

$$\tau_i^{\alpha\beta} = \frac{1}{2v_i} \sum_{j(\neq i)} f_{ij}^{\alpha}\, r_{ij}^{\beta}; \quad p_i = -\frac{1}{3} \sum_{\alpha=1}^{3} \tau_i^{\alpha\alpha} \qquad (2)$$

This relation implies the estimate of the local Voronoï volume $v_i$, associated with atom $i$. The Dirichlet-Voronoï regions [49, 50] can formally be simply defined in 2d as school districts if atoms represent schools [51]. The exact calculation of the Voronoï 3d volumes is somewhat involved [52]. The relative variation between this volume and that of a site in the perfect single crystal is $\Delta v_i/v = (v_i - v^\circ)/v^\circ$, where $v^\circ$ is the atomic Voronoï volume calculated in the perfect crystal.

## 2.4. Segregation energies and its driving forces

With the assumption of infinitely diluted solution, the segregation energy of a solute atom located at site $i$, $\Delta E_i^{\text{seg}}$, is calculated by the following formula

$$\Delta E_i^{\text{seg}} = E_i^{\text{tot}}(\text{solute}) - E_b^{\text{tot}}(\text{solute}) \qquad (3)$$

where $E_i^{\text{tot}}$ (solute) [resp. $E_b^{\text{tot}}$(solute)] is the total energy of the relaxed system with a solute atom located at

site $i$ [resp. located at a bulk site]. A negative value of the energy of segregation indicates that site $i$ is favourable to segregation. The sites to be considered here are atomic sites (substitution of a solvent atom by an atom of solute).

Segregation is modelled at the atomic scale not only to get numerical values but also with the aim of identifying its 'driving forces', that is to say the physical phenomena which can explain it. Wynblatt and Ku [25, 26] proposed for surface segregation a synthesis of the chemical approach of Defay and Prigogine developed for surfaces of liquids, with averaged first neighbours broken bonds [53] and the elastic approach of McLean developed for grain boundaries [54]. The energy of segregation was thus regarded as the sum of a "chemical" term due to the breaking of bonds and an "elastic" term due to the deformation elastic energy.

We showed in [24] that the Pines-Friedel formula used by McLean [54–57] works for a large solute atom in a slightly dilated atomic site or for a small solute atom in a slightly contracted atomic site, when such sites exist, but not for other cases. An atomistic level procedure adapted to FS-RGL potentials has been devised to define and calculate an elastic effect called size effect at atomic site $i$, $\Delta E_i^{\text{size}}$, as the energy of segregation including atomic relaxations of a virtual solute atom having all the parameters of the solvent except for the size which is taken equal to that of the impurity atom [21, 58].

In the original model of surface segregation which simply considers pair interactions between first neighbours on rigid lattices, the "chemical" term can be decomposed into two physical terms which can be calculated separately, one which corresponds to an excess cohesion energy effect per site and another one which corresponds to an "alloy" effect. This analysis has been extended to the many-body Finnis-Sinclair type potentials [27]. One can also heuristically let the computer relax the rigid lattice condition. The resulting three driving force analysis has thus been rather successfully applied to surface segregation studies using reasonably realistic FS-RGL2 potentials [21, 22]. It has also been extrapolated to GB segregation [21, 22] with the numerical observation that the "alloy" effect should not be considered at least in the way it was estimated. One of us showed that the artificial decomposition of the chemical term into an excess cohesion energy effect and an "alloy" effect is actually not justified analytically in the infinite dilution limit even within the simplest models for grain boundary segregation [59]. No alloy effect is expected and one is left with a chemical effect which can only be tentatively assimilated to an excess cohesion energy term.

One thus only has two driving forces for GB segregation, with a tentative phenomenological decomposition as following

$$\Delta E_i^{\text{seg}} = \Delta E_i^{\text{size}} + \Delta e_i^{\text{xscoh}} \tag{4}$$

The elastic size effect is calculated by the method of virtual impurity which was mentioned above [21, 58].

The cohesion effect corresponds to a difference in excess cohesion energies of site $i$, defined in the following way for a system $M(I)$

$$\Delta e_i^{\text{xscoh}}[M(I)] = e_i^{\text{xscoh}}(I) - e_i^{\text{xscoh}}(M) \tag{5}$$

where $e_i^{\text{xscoh}}(A)$ represents the excess cohesive energy of site $i$ for an atom in pure system $A$, $e_i^{\text{xscoh}}(A) =$

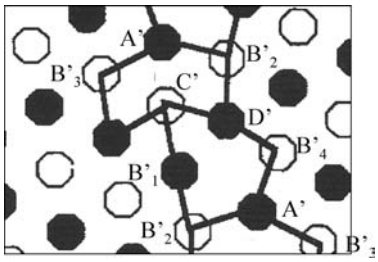


*Figure 2* Structure of the $\Sigma 11'$ {332} ⟨110⟩ grain boundary as simulated in nickel. See [62] for the comparison with the experimental image. The labelling of sites is explicited in the following Section.

TABLE II Geometrical and physical characteristics of the principal sites of {332} grain boundary in pure metals

| | Ni | | | Cu | | |
|---|---|---|---|---|---|---|
| Site | $\Delta v_i/v$ (%) | $p_i$ (GPa) | $e_i^{\text{xscoh}}$ (meV) | $\Delta v_i/v$ (%) | $p_i$ (GPa) | $e_i^{\text{xscoh}}$ (meV) |
| $A'$ | 11.2 | −10.5 | 62 | 10.69 | −6.7 | 41 |
| $B'_1$ | 9.0 | −1.61 | 165 | 8.77 | −1.57 | 103 |
| $B'_2$ | 3 | −3.27 | 50 | 2.53 | −2.0 | 30 |
| $B'_3$ | 2.2 | −3.6 | 9.5 | 2.28 | −2.34 | 5 |
| $B'_4$ | 2.85 | 2.55 | 138 | 2.61 | 1 .44 | 88 |
| $C'$ | −0.8 | 2.86 | 73 | −0.92 | 1.70 | 45 |
| $D'$ | −0.2 | 11.11 | 270 | −0.49 | 6.69 | 171 |
| | Ag | | | Au | | |
| $A'$ | 11.4 | −4.38 | 55 | 10.85 | −5.4 | 68 |
| $B'_1$ | 9.8 | −0.60 | 101 | 10.0 | −0.6 | 110 |
| $B'_2$ | 4.5 | −2.55 | 29 | 5.36 | −4.0 | 38 |
| $B'_3$ | 1.8 | −1.27 | 5.6 | 1.3 | −1.28 | 6.4 |
| $B'_4$ | 4.1 | 0.77 | 71 | 4.86 | 0.6 | 71 |
| $C'$ | −.96 | 1.14 | 30 | −1.15 | 1.7 | 29 |
| $D'$ | 1.1 | 4.67 | 140 | 1.75 | 5.62 | 142 |

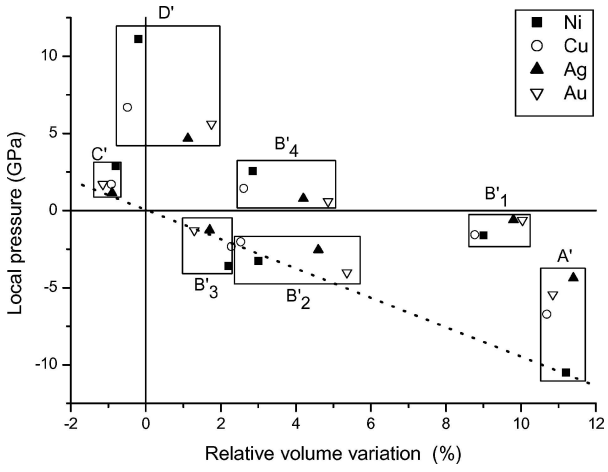


*Figure 3* Pressures $p_i$ (Gpa) versus the volume variations $\Delta v_i/v$ (%) for the seven significant intergranular atomic sites of the {332} GB for the four metals, Ni, Cu, Ag and Au. The dotted line is mainly a guide for the eye. Sites $B'_1$, $B'_4$ and $D'$ clearly appear as off that line.

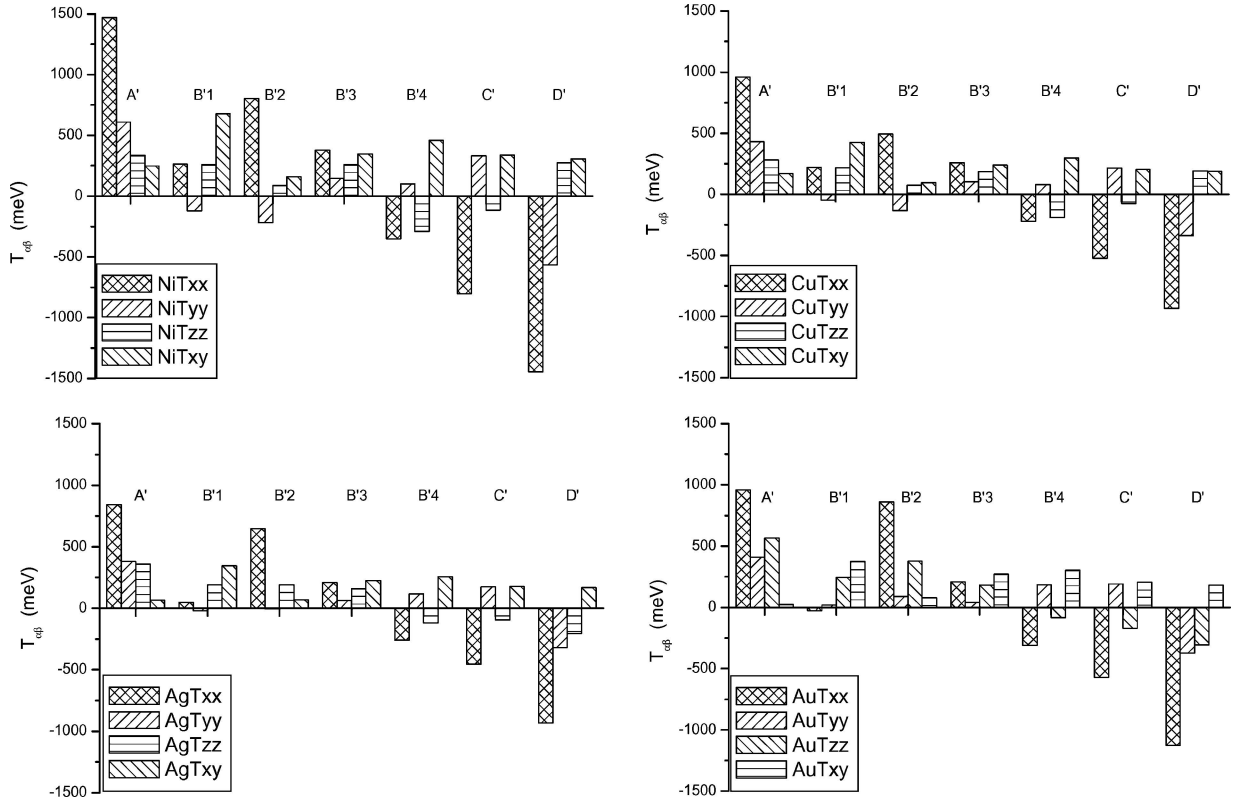


*Figure 4* Components of the local stress tensors per atomic site for the four metals Ni, Cu, Ag and Au. We give here $T_{\alpha\beta}(\text{site}) \equiv v_i$, $\tau_i^{\alpha\beta}$ in meV, one has $T_{\alpha\beta}(\text{site}) \sim v^\circ \tau_i^{\alpha\beta}$ (and $v^\circ = a^3/4$). With respect to Fig. 2, $x$ is vertical ($\langle 113 \rangle$) and $y$ is horizontal ($\langle 332 \rangle$). Because each site appears twice in the structure we only give the absolute value of $T_{xy}$. Out of plane $T_{xz}$ and $T_{yz}$ components have zero values.

$E_i(A) - E_{\text{coh}}(A)$, where $E_i(A)$ is the cohesive energy of the $i$ site atom.

It is the validity of this decomposition which will be checked in the following for various systems.

## 3. Σ11′ {332} ⟨110⟩ grain boundary segregation

### 3.1. Atomic structure

This GB has been studied and observed on the atomic level with perfect agreement between the atomic simulations [60, 61] and the HRTEM observations in a nickel bicrystal [62]. The atomic structure is not symmetric in the immediate vicinity of the {332} interfacial plane. Its local structural pattern is named "zigzag" with a symmetry of second kind of the type m' characterized by a glide mirror plane, cf. Fig. 2. At larger distances from the grain boundary plane, this grain boundary is also characterized by a vertical rigid translation between the grains by ∼0.4 the {113} interplanar distance. It should be noted that it is not this translation which confers the m' symmetry to this grain boundary, contrary to the case of Σ3 {112} studied by Menyhard *et al.* [13]. The Σ11′ {332} GB is a grain boundary of high energy. Its calculated energy is approximately twice that of the Σ11 {113} GB [62]. The excess interfacial energies of the optimised structures are, in mJ/m$^2$, 967.8 for Ni, 580.5 for Cu, 399.5 for Ag and 434.4 for Au. Although these excess energies do not have to be proportional to the bulk cohesive energies of the corresponding materials given in Table I (compare with [63]), the inversion in this respect between copper and gold is essentially due to the difference of the crystallographic parameters since these excess energies are actually given per surface units (also see [64]). In addition to the importance of the agreement between numerical simulation and experimental observations, at least in the case of nickel, the structure of this grain boundary has the advantage of being stable, in particular with respect to segregation. We did check for everyone of the four potentials that the zigzag glide mirror plane structure is the stable structure with respect to the quasi mirror symmetric structure M also studied in [65].

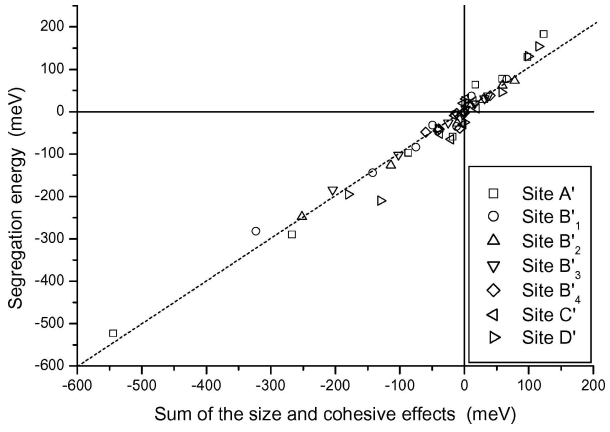


*Figure 5* Plot of the segregation energies $\Delta E_i^{\text{seg}}$ versus the sums of the size effect and the excess cohesion effect $\Delta E_i^{\text{size}} + \Delta e_i^{\text{xscoh}}$ per atomic site for all studied systems.

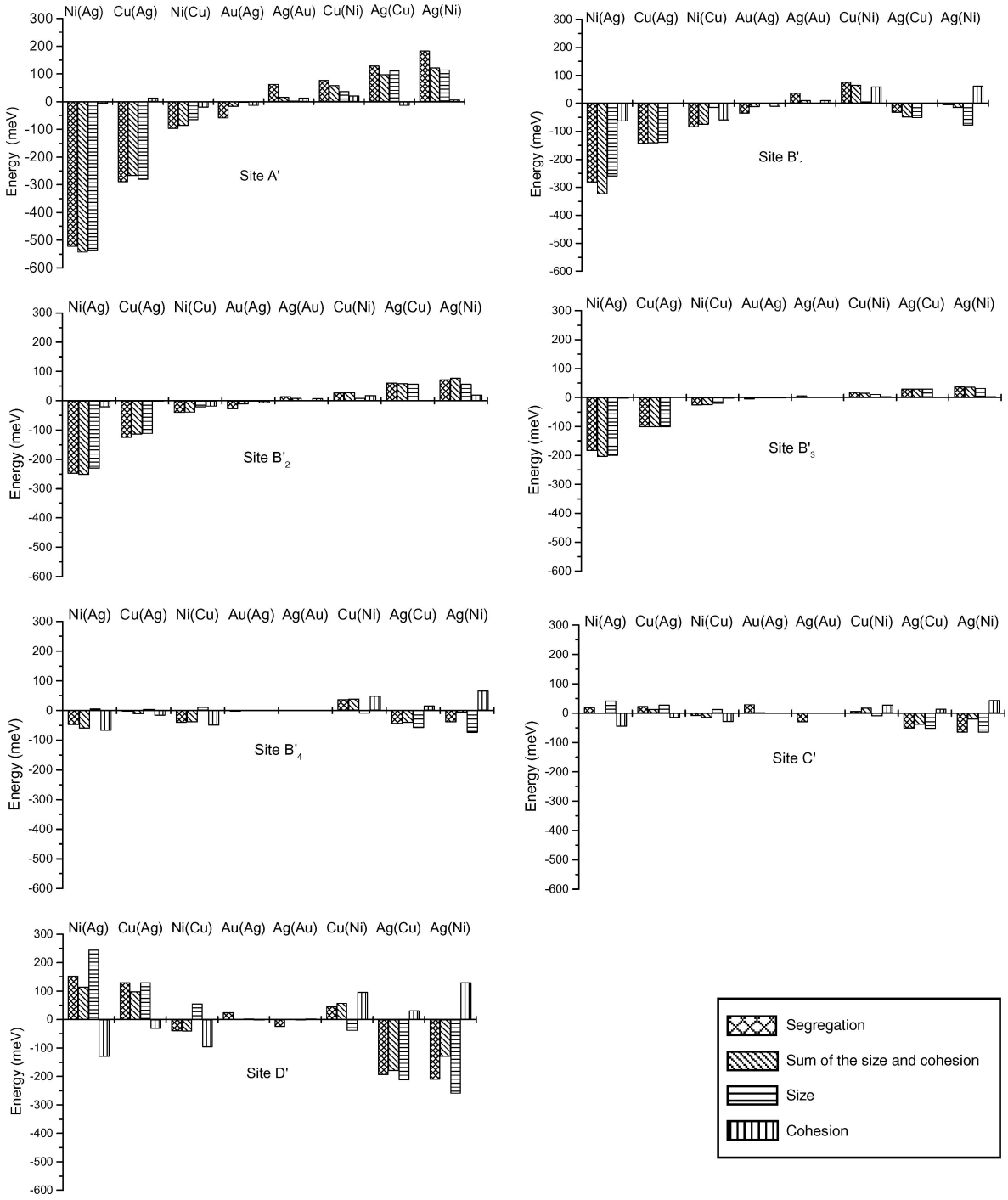


*Figure 6* Segregation energy balance detailed by site and binary alloy.

## 3.2. Characterization of the principal sites and their physical properties

Seven types of significant atomic sites can be identified. They are denoted as in [24], v.g. according to the order of their segregation energy in the direct Ni(Ag) system for which these energies have the strongest values: $A'$, $B'_1$, $B'_2$, $B'_3$, $B'_4$, $C'$ and $D'$ (see Fig. 2). Above mentioned geometrical and physical properties of these intergranular sites have been calculated in each pure metallic system and are compiled in Table II.

The relative volume variations $\Delta v_i/v$ remain essentially similar for all the considered metals with nevertheless possible non-negligible relative differences, in particular for the $B'_2$, $B'_4$ and $D'$ sites. One observes in Fig. 3 a good correlation between $p_i$ and $\Delta v_i/v$ except for the $B'_1$, $B'_4$ and $D'$ sites. It is noteworthy that these three sites have relatively important excess cohesive energies in each of the four metals. Examination of the local stress tensor components in Fig. 4 shows that the hydrostatic condition is almost never satisfied and that the planar $T_{xy}$ off-diagonal component often has a value comparable with those of the diagonal components. Sites $A'$ and $D'$ are hydrostatic-like, $A'$ strongly in tension, $D'$ strongly in compression. The other sites are highly non hydrostatic. Although $A'$ is as much in tension as $D'$ is in compression, the excess cohesive energies are much smaller for $A'$ than for $D'$. This reflects the anharmonic character of the interatomic potentials. Large compressions are energetically more costly than large extensions.

### 3.3. Analysis and discussion of the segregation driving forces

Fig. 5 shows that the sum of both the size and cohesion effects always allows a good reproduction of the segregation energy per atomic site in all binary systems studied here. The phenomenological analysis developped in Section 2.4 which leads to equation 7 is thus corroborated by numerical calculations on binary metallic systems with embedded atom potentials.

To allow for a more detailed analysis, the balance of the segregation energies versus the driving effects is explicited in Fig. 6.

The size effect clearly appears as the main driving force for segregation for systems like Ni(Ag) and Cu(Ag) for which the atomic size difference $|r-1|$ is indeed greater than 10%.

The Ni(Cu) (and its reverse Cu(Ni)) system is interesting in as much as it corresponds to a case where the size effect is small ($|r-1| \sim 2\%$) and the excess cohesion effect can play a major role. This is specially the case for sites $B_1'$, $B_4'$ and $D'$ where the size effect is small with respect to the excess cohesion effect, (this is also true for site $C'$ although with small values and negligible segregation energies). $B_1'$ and $B_4'$ undergo a large shear stress ($T_{xy}$, see Fig. 2) and $D'$ is strongly compressed. The excess cohesive energies being much smaller for $A'$ than for $D'$, as explained in Section 3.2, the excess cohesion effect is negligible for the $A'$ site which is not the symmetric of the D′ site from that point of view.

The excess cohesion effect also plays an important rôle for these $B_1'$, $B_4'$ and $D'$ sites in Ni(Ag) (and Ag(Ni)), even if the size effect is very strong in these systems.

The fact that in systems containing nickel, the excess cohesive effect is important for anisotropically disturbed sites like $B_1'$ and $B_4'$ can be related to the fact that nickel is the only transition metal among the four metals considered here. As seen in Table I (Section 2.1), nickel is much more resistant to shear stresses than copper, silver and gold, a feature that our potentials reproduce reasonably well. The site $D'$ also undergoes some local shear stress coupled to its strongly compressed state.

For systems with no size effect such as Au(Ag) and Ag(Au), which have a size difference of only 0.2%, all effects are very small and cannot be discussed further. Besides the non relativistic limitation of our semi-empirical potential already alluded to at the end of Section 2.1, one should also mention that the Au-Ag deviation from Vegard's law follows the Zen's law [66] and cannot be explained with simple modellisations [55, 67, 68].

We checked that we obtained similar behaviours per atomic site in the case of the $\Sigma 11$ {113} grain boundary except for the fact that this latter has no strongly compressed site.

## 4. Conclusions

The segregation energy numerically analysed in the infinitely diluted limit at the atomic level appears to be essentially given by the sum of a size effect and an excess cohesion effect for all binary metallic systems made of nickel, copper, silver and gold. The size effect is often the predominant effect. This soundly generalises previous conclusions drawn from limited studies.

It is however found that for non hydrostatic and/or strongly compressed atomic sites the contribution of the excess cohesion effect can be important. This effect can even be the leading one for such sites when one of the metals is the transition one, nickel, and the other is a noble metal as copper. We relate this behaviour to the special character of these sites coupled to the rigid d-binding of nickel versus the soft s-binding of noble metals.

We believe that the excess cohesion effect can also be important when the solute and the solvant are of a very different nature, such as for sulfur in nickel or phosphorous in iron which are cases of concern in industrial applications.

## Acknowledgements

This research has been supported by a CNRS-ASRT cooperation program (projets 12139 and 14681). We thank B. Legrand (CEA, Saclay), G. Tréglia (CRMC2, Marseille), F. Berthier, R. Tétot (LEMHE, Orsay), J. Creuze (LURE, Orsay), V. Pontikis, L. Priester (CECM, Vitry), and P. Lejcek (IoP, Prague) for their sustained interest in this work and for frequent and fruitful discussions. One of us (OHD) also acknowledges peripatetic discussions with P. Wynblatt (CMU, Pittsburgh) at iib2004 in Belfast.

## References

1. R. W. BALLUFFI, in "Interfacial Segregation", edited by W. C. Johnson and J. M. Blakely (American Society for Metals, Metal Park, Ohio, 1979) p. 193.
2. C. L. BRIANT, in "Materials Interfaces: Atomic-level Structures and Properties," edited by D. Wolf and S. Yip (Chapman & Hall, London, 1992) p. 463.
3. S. M. FOILES and D. N. SEIDMAN, in "Materials Interfaces: Atomic-level Structures and Properties," edited by D. Wolf and S. Yip (Chapman & Hall, London, 1992) p. 497.
4. P. LEJCEK and S. HOFMANN, *Crit. Rev. Sol. St. Mat. Sci.* **20** (1995) 1.
5. A. P. SUTTON and R. W. BALLUFFI, in "Interfaces in Crystalline Solids" (Oxford University Press, New York, 1995).
6. E. D. HONDROS, M. P. SEAH, S. HOFFMAN and P. LEJCEK, in "Physical Metallurgy," 4th, revised, edn, edited by R. W. Cahn and P. Haasen (North Holland, Amsterdam, 1996) Vol. II, p. 1201 .
7. A. P. SUTTON and V. VITEK, *Acta Metall.* **30** (1982) 2011.
8. D. WOLF, in "Character of Grain Boundaries," Advances in Ceramics, edited by M. F. Yan and A. H. Heuer (The American Ceramic Society, Inc., Colombus, 1983) Vol. 6.
9. V. VITEK and G. J. WANG, *Surf. Sci.* **144** (1984) 110.
10. M. HASHIMOTO, Y. ISHIDA, S. WAKAYAMA, R. YAMAMOTO, M. DOYAMA and T. FUJIWARA, *Acta metall.* **32** (1984) 13.
11. A. LARERE, K. I. MASUDA-JINDO, R. YAMAMOTO and M. DOYAMA, in "Grain Boundary Structure and Related Phenomena," Proceedings of JIMIS-4 (The Japan Institute of Metals, Sendai, 1986) p. 229.
12. T. A. ARIAS and J. D. JOANNOPOULOS, *Phys. Rev. Lett.* **69** (1992) 3330.
13. M. MENYHARD, MIN YAN and V. VITEK, *Acta Metall. Mater.* **4** (1994) 2783.

14. A. MAITI, M. F. CHILSHOLM, S. J. PENNYCOCK and S. T. PANTELIDES, *Phys. Rev. Lett.* **77** (1996) 1306.
15. H. HUANG, T. DIAZ DE LA RUBIA and M. J. FLUSS, *Mater. Res. Soc. Symp. Proc.* **428** (1996) 177.
16. J. D. RITTNER and D. N. SEIDMAN, *Acta mater.* **45** (1997) 3191.
17. D. UDLER and D. N. SEIDMAN, *ibid.* **46** (1998) 1221.
18. X.-Y. LIU, W. XU, S. M. FOILES and J. B. ADAMS, *Appl. Phys. Let.* **71** (1998) 1578.
19. L. G. WANG and C. Y. WANG, *Mater. Sci. Forum* **294–296** (1999) 489.
20. W. T. GENG, A. J. FREEMAN, R. WU, C. B. GELLER and J. E. RAYNOLD, *Phys. Rev. B* **60** (1999) 7149 .
21. F. BERTHIER, B. LEGRAND and G. TRÉGLIA, *Acta Mater.* **9** (1999) 2705.
22. J. CREUZE, *Defect and Diffusion Forum* **203–205** (2002) 3.
23. R. JANISCH and C. ELSÄSSER, *Phys. Rev. B* **67** (2003) 224101.
24. B. LEZZAR, O. KHALLFALLAH, A. LARERE, V. PAIDAR and O. HARDOUIN DUPARC, *Acta mater.* **52** (2004) 2809.
25. P. WYNBLATT and R. C. KU, *Surf. Sci.* **65** (1977) 511.
26. *Idem.*, in "Interfacial Segregation," edited by W. C. Johnson and J. M. Blakely (ASM, Metals Park, Ohio, 1979) p. 115.
27. G. TRÉGLIA, B. LEGRAND and F. DUCASTELLE, *Europhys. Lett.* **7** (1988) 575.
28. F. DUCASTELLE, B. LEGRAND and G. TRÉGLIA, *Suppl. Prog. Theor. Phys.* **101** (1990) 159.
29. R. HULTGREN, P. D. DESAY, D. T. HAWKINS, M. GLEISER and K. K. KELLY (Eds.), in "Selected Values of the Thermodynamic Properties of Metals and Binary Alloys" (John Wiley, New York, 1973).
30. T. B. MASSALSKI (Ed.), in "Binary Alloys Phase Diagrams" (American Society for Metals, Metal Park, Ohio, 1986).
31. W. HUME ROTHERY, *J. Inst. Metals* **35** (1926) 295. Also see his "Atomic Theory for the Students of Metallurgy" (The Institute of Metals, London, 1955, 1960).
32. M. W. FINNIS and J. E. SINCLAIR, *Phil. Mag.* **A50** (1984) 45.
33. V. ROSATO, M. GUILLOPÉ and B. LEGRAND, *ibid.* **A59** (1989) 321.
34. C. KITTEL, in "Introduction to Solid State Physics" 7th (ed.), (John Wiley & Sons, Inc., New York, 1996).
35. M. S. DAW and M. I. BASKES, *Phys. Rev. B* **29** (1984) 6443.
36. J. FRIEDEL, in "The Physics of Metals," edited by J. M. Ziman (Cambridge University Press, Cambridge, England, 1978) p. 341.
37. G. J. ACKLAND, G. TICHY, V. VITEK and M. W. FINNIS, *Phil. Mag.* **A56** (1987) 735.
38. J. H. ROSE, J. FERRANTE and J. R. SMITH, *Phys. Rev. Lett.* **47** (1981) 675.
39. H. J. WOLLENBERGER, in *Physical Metallurgy*, 4th revised, edn., edited by R. W. Cahn and P. Haasen (Elsevier Science, Amsterdam, 1996), p. 1621.
40. L. E. MURR, in "Interfacial Phenomena in Metals and Alloys" (Addison-Wesley, Reading, Massachusetts, 1975).
41. D. J. H. COCKAYNE, M. L. JENKINS and I. L. F. RAY, *Phil. Mag.* **24** (1971) 1383 .
42. M. L. JENKINS, *ibid.* **A26** (1972) 747.
43. J. EYMERY, F. LANCON and L. BILLARD, *J. Phys. I France* **3** (1993) 787.
44. P. PYYKKÖ, *Chem. Rev.* **97** (1977) 597.
45. P. PYYKKÖ and J. P. DESCLAUX, *Accounts of Chem. Res.* **12** (1979) 276.
46. J. R. BEELER JR. and G. L. KULCINSKI, in "Interatomic Potentials and Simulations of Lattice Defects," edited by P. C. Gehlen, J. R. Beeler Jr. and R. I. Jaffe (Plenum Press, New York, 1972) p. 735.
47. O. HARDOUIN DUPARC and M. TORRENT, *Interf. Sci.* **2** (1994) 7 .
48. V. VITEK and T. EGAMI, *Phys. Stat. Sol.* **B144** (1987) 145.
49. G. P. LEJEUNE DIRICHLET, *Journal fur die reine und angewandte Mathematik* **40** (1850) 209.
50. G. F. VORONOÏ, *Journal für die reine und angewandte Mathematik* **133** (1908) 97; *ibid.* **134** (1908) 198; *ibid.* **136** (1909) 67.
51. J. H. CONWAY and N. J. A. SLOANE, in "Sphere Packings, Lattices and Groups" (Springer-Verlag, New York, 1993).
52. B. C. RAPAPORT, in "The Art of Molecular Dynamics" (Cambridge University Press, Cambridge, 1995).
53. R. DEFAY and I. PRIGOGINE, in "Tension Superficielle et Adsorption" (Desoer, Liege, 1951); with A. Bellemans, translated by D. H. Everett, Surface Tension and Adsorption (Longmans, London, 1966).
54. D. MCLEAN, in "Grain Boundaries in Metals" (Oxford University Press, London, 1957).
55. B. J. PINES, *J. Phys.* (Moscow, Acad. USSR) **3** (1940) 309.
56. J. FRIEDEL, *Advan. Phys.* **3** (1954) 446.
57. J. D. ESHELBY, *Adv. Solid State Phys.* **3** (1956) 79.
58. G. TREGLIA and B. LEGRAND, *Phys. Rev. B* **35** (1987) 4338.
59. O. HARDOUIN DUPARC, not yet published note.
60. J. D. RITTNER and D. N. SEIDMAN, *Phys. Rev. B.* **54** (1996) 6999.
61. V. PAIDAR, A. LARERE and L. PRIESTER, in "Interface Science and Materials Interconnection," in Proceedings of JIMIS-8 (The Japan Institute of Metals, Sendai, 1997) p. 523.
62. O. HARDOUIN DUPARC, S. POULAT, A. LARERE, J. THIBAULT and L. PRIESTER, *Phil. Mag.* **A80** (2000) 853 .
63. E. S. MACHLIN, *Scripta Metall.* **14** (1980) 125.
64. D. UDLER and D. N. SEIDMAN, *Phys. Rev. B* **54** (1996) 11133.
65. A. LARERE, M. GUILLOPE and K. I. MASUDA-JINDO, *J. Phys. Colloq. France* **49** (1988) C5-47.
66. E. ZEN, *Amer. Mineral.* **41** (1951) 523.
67. J. FRIEDEL, *Phil. Mag.* **46** (1955) 514.
68. C. D. GELATT and H. EHRENREICH, *Phys. Rev. B* **10** (1974) 398.


*Received 19 September 2004*
*and accepted 31 January 2005*